

## RESEARCH ARTICLE

# Direct monitoring of drug-induced mechanical response of individual cells by atomic force microscopy

Van-Chien Bui<sup>1,2</sup> | Thi-Huong Nguyen<sup>1,3</sup> <sup>1</sup>Institute for Immunology and Transfusion Medicine, University Medicine Greifswald, Greifswald, Germany<sup>2</sup>ZIK HIKE, University of Greifswald, Greifswald, Germany<sup>3</sup>Institute for Bioprocessing and Analytical Measurement Techniques, Heilbad Heiligenstadt, Germany**Correspondence**Dr. Thi-Huong Nguyen, Institute for Bioprocessing and Analytical Measurement Techniques, Rosenhof 1, 37308 Heilbad Heiligenstadt, Heiligenstadt, Germany  
Email: thi-huong.nguyen@iba-heiligenstadt.de  
Phone: +49(0)3606671600  
Fax: +49(0)3606671200**Funding information**

German Federal Ministry of Education and Research (BMBF), Grant/Award Number: FKZ 03Z2CN12; German Research Foundation, Grant/Award Numbers: DFG, NG 133/1-2

**Abstract**

Mechanical characteristics of individual cells play a vital role in many biological processes and are considered as indicators of the cells' states. Disturbances including methyl- $\beta$ -cyclodextrin (M $\beta$ CD) and cytochalasin D (cytoD) are known to significantly affect the state of cells, but little is known about the real-time response of single cells to these drugs in their physiological condition. Here, nanoindentation-based atomic force microscopy (AFM) was used to measure the elasticity of human embryonic kidney cells in the presence and absence of these pharmaceuticals. The results showed that depletion of cholesterol in the plasma membrane with M $\beta$ CD resulted in cell stiffening whereas depolymerization of the actin cytoskeleton by cytoD resulted in cell softening. Using AFM for real-time measurements, we observed that cells mechanically responded right after these drugs were added. In more detail, the cell's elasticity suddenly increased with increasing instability upon cholesterol extraction while it is rapidly decreased without changing cellular stability upon depolymerizing actin cytoskeleton. These results demonstrated that actin cytoskeleton and cholesterol contributed differently to the cell mechanical characteristics.

**KEYWORDS**

atomic force microscopy, cell elasticity, HEK cells, nanoindentation, stiffness

## 1 | INTRODUCTION

Mechanical properties of cells play an important role in various biological processes including cell migration, growth, proliferation, or division.<sup>1-3</sup> It can reflect changes in the chemical medium<sup>4</sup> and is dependent on various factors such as microridges, microvilli, and cilia,<sup>5</sup> actomyosin,<sup>6</sup> or salts.<sup>4,7</sup> Several methods including optical stretcher,<sup>8</sup> micropipette aspiration,<sup>9</sup> and atomic force microscopy (AFM),<sup>10</sup> are commonly used to measure mechanical properties of cells in the adherent or suspended states over a wide range of physiological conditions. Optical traps and micropipette aspiration are always utilized for suspended cells while AFM is used for substrate-anchored or adherent cells. Among these techniques, AFM has been widely used to directly measure the mechanics of substrate-anchored

or substrate-adherent cells with a high spatial resolution ( $\sim 1$  nm) and sensitivity ( $\sim 1$  pN) under physiological cell culture environments.<sup>11,12</sup> The elastic response to the external force of individual cells is normally characterized by an established contact model derived from continuum mechanics (Hertz model).<sup>13</sup> This model describes the elastic deformation of a homogenous continuum with a spherical indenter in the absence of adhesion and is proved to be useful to get an overall bulk elasticity of the measured cells.<sup>14,15</sup>

The shape of cells is formed by a connection of a cell membrane with an actin cortex (also called actomyosin cortex) via various proteins like those belonging to the ezrin/radixin/moesin (ERM) protein family.<sup>16,17</sup> Cell membrane mainly formed by proteins and lipids is the outermost layer that envelopes cytoplasm of the cell and protects the cell integrity along with supporting and maintaining the cell's shape. It

This is an open access article under the terms of the Creative Commons Attribution License, which permits use, distribution and reproduction in any medium, provided the original work is properly cited.

© 2020 The Authors. *Journal of Molecular Recognition* published by John Wiley & Sons Ltd.

plays a key role in regulating cell function and controlling the movement of substances in and out of the cell. It also protects the cell from external environment and participate in various cellular processes such as cell adhesion, signal transduction, energy conversion, ion conductivity, cellular transport, survival, surface recognition, or proliferation.<sup>18,19</sup> Cellular characteristics and functions can be directly affected by any change in the structure of the cell membrane.<sup>20,21</sup> One of the main components of the plasma membrane in all mammalian cells is cholesterol where cholesterol/phospholipids molar ratio may be as high as 1:1.<sup>22</sup> Changes in the level of cholesterol in the plasma membrane are known to have a major impact on the physical properties of the membrane lipid bilayer, such as changes in membrane fluidity, ordering of the phospholipids, and membrane deformability (elasticity).<sup>23</sup> Actin cortex, formed by an actin-rich network consisting of F-actin filaments, actin-binding proteins, and myosin motors,<sup>24,25</sup> is a cytoplasmic protein layer attached to the inner side of the cell membrane via membrane-anchoring ERM proteins. The dynamic alteration of the actomyosin plays a major role in cellular processes associated with cell shape remodeling and cellular contraction, as well as modulating membrane behavior and surface mechanical properties.<sup>17,26</sup>

The diverse interplay between the plasma membrane and the cell cortex requires a well-established biological model with limited disturbance from cell migration, growth, and proliferation. Although the cell mechanical characteristics are significantly affected by changes in membrane cholesterol<sup>23,27</sup> or actin contents,<sup>28-31</sup> the real-time mechanical response of the cell against the devoid of these composition remains unclear. The goal of this study is to understand the impact of cholesterol and actin in the deformability of the membrane-cytoskeleton complex.

Here, we use nanoindentation-based AFM to directly monitor the mechanical response of the human embryonic kidney (HEK) cells, a cell line transformed with adenovirus<sup>32</sup> that shows cancer-like behavior in tissue culture, upon depletion of the membrane cholesterol and/or disruption of the actin cytoskeleton. Although the mechanical characteristics of HEK have been investigated, there is still a large variation in the reported results. Kagiwada and coworkers used a 200 nm-diameter nanoneedle for nanoindentation measurements reported that HEK cell elasticity is  $6.5 \pm 2.5$  kPa<sup>33</sup> while Shimizu and coworkers used spherical tip for AFM experiments and reported that HEK cell elasticity is  $\sim 0.4$  kPa.<sup>34</sup> As a result, we first reexamined the elasticity of the untreated cells and used as a control and then investigated the effect of the disruption of membrane cholesterol by methyl- $\beta$ -cyclodextrin (M $\beta$ CD) and of the depolymerization of actin cortex by cytochalasin D (cytoD) on cell mechanics in real-time.

## 2 | MATERIALS AND METHODS

### 2.1 | Cell preparation

About 24 mm round glass coverslips (Plano GmbH, Wetzlar, Germany) were sonicated in turn in acetone, ethanol, and DI water for 5 minutes. The coverslips were then dried under a nitrogen stream, immersed into

0.02% poly-L-lysine (PLL) (Sigma Aldrich, Hamburg, Germany) for 30 minutes, and dried again with N<sub>2</sub> blow. HEK293T cells (Life Technologies, Darmstadt, Germany) were trypsinized by 0.25% Trypsin-0.02% EDTA (PAA-BioPharm, Darmstadt, Germany) in PBS for 2 minutes at 37°C followed by rinsing with PBS (PAA-BioPharm, Darmstadt, Germany). Cells were cultured on PLL-coated coverslips placed in a sterilized six well plate in Dulbecco's-modified Eagle's medium (DMEM) (Pan-Biotech) supplemented with 1% Penicillin/Streptomycin, 1% L-glutamine and 10% heat-inactivated fetal calf serum (PAA-BioPharm, Darmstadt, Germany) at 37°C under a 5% CO<sub>2</sub> humidified atmosphere for 5 hours prior to experiments. Actin cytoskeleton depolymerization and cholesterol extraction were induced by treating the cells with cytoD and M $\beta$ CD (Sigma-Aldrich, Steinheim, Germany).

### 2.2 | Force measurements

Force measurements on HEK cells were carried out in cell culture medium at 37°C by Nano Wizard 3 AFM (JPK Instruments AG, Berlin, Germany) combined with an inverted microscope (Olympus IX 81, objective 20x/0.45). This combination allows the AFM probe to be positioned on any region of interest of the cell surface. A commercial 5  $\mu$ m silica bead was attached to the end of a backside gold-coated Si<sub>3</sub>N<sub>4</sub> tipless cantilever (model MLCT-O10, Bruker AFM Probes, Camarillo, CA) by the glue NOA68 (Norland Products) under short wavelength UV light (254 nm) for 15 minutes followed by exposing to oxygen plasma for 1 minute to remove organic components. The actual bead size of  $4.2 \pm 0.05$   $\mu$ m was measured again by scanning electron microscopy (SEM) (Carl Zeiss AG, Jena, Germany). The spring constant of the cantilevers of  $12 \pm 2$  pN/nm was calibrated right before each measurement using the thermal noise method (JPK Instruments AG). This cantilever was used for all measurements with a tip speed of 2 curves/s and a loading force of 150-200 pN. Other parameters were optimized for the measurements. To evaluate the mean elasticity of cells, 64 to 100 force vs distance (F-D) curves were recorded on top (nuclear region) of single cells and 100 untreated cells, 91 cells preincubated with 10 mM M $\beta$ CD for 2 hours, and 103 cells preincubated with 10  $\mu$ M cytoD for 30 minutes were collected. To directly monitor the cell response, the drugs were added during elasticity measurements on untreated cells. F-D curves were then converted to force vs indentation curves, which were the slope difference of the F-D curves measured on top of the cell and on a glass surface, followed by fitting with Hertz model<sup>13,35</sup> using Equation 1:

$$F = \frac{4E\sqrt{R}}{3(1-\nu^2)}\delta^{\frac{3}{2}} \quad (1)$$

where R is the radius of the bead,  $\delta$  is the indentation depth, and  $\nu$  is Poisson's ratio (assumed to be 0.5 for a soft sample) to calculate elasticity E of the cell. These processes were carried out with JPK data processing software version spm-4.4.18+. Data analyses were done with origin software (version 9.1, Origin Lab Corporation, Northampton, MA, USA).

### 3 | RESULTS

To examine the mechanical properties of cells, we prepared AFM spherical tips and cells for nanoindentation experiments by AFM (Figure 1). Figure 1A shows an SEM image of a spherical bead firmly stuck to the end of an AFM tipless cantilever which was used to indent the cells. Figure 1B shows a model for nanoindentation measurement on adherent cell cultured on PLL coated glass substrates. Applying a force  $F$  to the cell when the bead is in contact with the cell surface will help the bead to indent the cell and make cantilever bent. This bending of the cantilever will be recorded by AFM and will serve as input parameters of the F-D curve (Figure 1C). The difference between force curves measured on the hard glass and soft cell surfaces shows the deformation of the cell under the tip load, that is, how much the tip indents the cell. This deformation will be converted into force-indentation curves which will then be fitted with the Hertz model to calculate Young's modulus of the cell.

Figure 1D is an overlay of the fluorescence and optical image showing the silhouette of an AFM cantilever end carrying silica bead placed on the top (nuclear region, blue) of a cell for force measurements. An important parameter in nanoindentation measurement is

the height of the sample of interest. It is said that if the indentation depth exceeds 10% of the cell height, the complication of the underlying hard substrate should be taken into account.<sup>36</sup> Therefore, we measured the cell height by approaching the cell top and glass surface to the bead and recorded the cantilever position on these two surfaces (total five cells, ranging from smallest to largest cells). The measured difference of the cantilever position on top of the cell and on the glass surface is 6 to 10  $\mu\text{m}$  which is approximately equal to the cell height.

Figure 2 shows the elasticity measurement of the HEK cell. Figure 2A is a representative force-indentation curve with an indentation depth  $<10\%$  of the cell height derived from an F-D curve measured on a cell using AFM data processing software. To verify the stability of single cells, we continuously measured the elasticity on top of individual cells and observed that the elasticity of single cells varies in a range of around 400 Pa, but the median elasticity remains stable for more than 30 minutes (Figure 2B). The corresponding mean elasticity of individual cells is shown in Figure 2C. The error bar on each data point is a SE of the mean (s.e.m). Figure 2D presents the elasticity histogram which is fitted with a Gaussian dispersion model (solid line) to get the mean elasticity  $\pm$  s.e.m of 100 cells of  $259.3 \pm 8.6$  Pa.

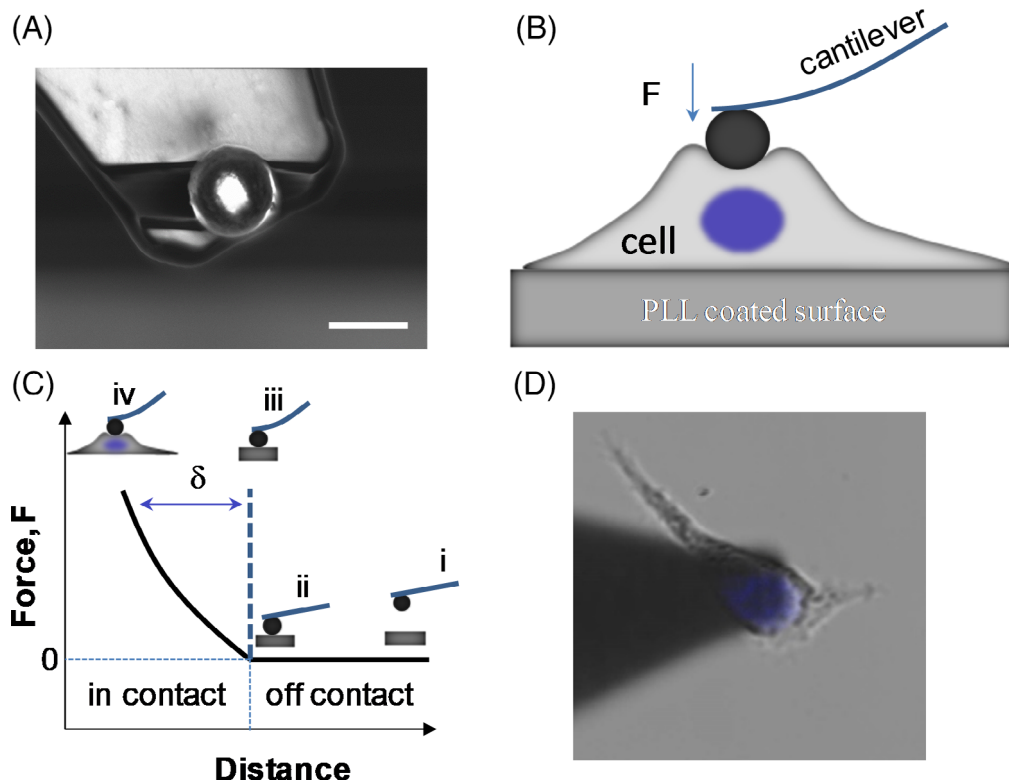


**FIGURE 1** Measuring cellular mechanics by nanoindentation-based AFM. A, SEM image showing a silica bead glued at the end of an AFM cantilever. Scale bar is 4  $\mu\text{m}$ . B, Cartoon showing the force measurement on a cell on PLL-coated glass substrate. C, Schematic showing an approaching force vs distance curve measured on hard glass (dashed line) and cell (solid line) surface by AFM. When the tip is far from the sample surface, the cantilever is not bent (i) and therefore no change in the force can be observed. Upon contact with the surface (ii), the cantilever starts to bend, and the force starts to increase. On the hard glass surface, the bending of the cantilever (iii) is proportional to the extension of the AFM piezo stage while on soft cell surface the bending of the cantilever (iv) will follow an inward course. The difference of the force curves measured on these two surfaces corresponds to the indentation depth ( $\delta$ ) of the cell. D, Overlay of the fluorescence and bright-field images showing a silhouette of an AFM cantilever on top of an adherent cell. Blue region is nuclear of the cells labeled by DNA dye DRAQ5

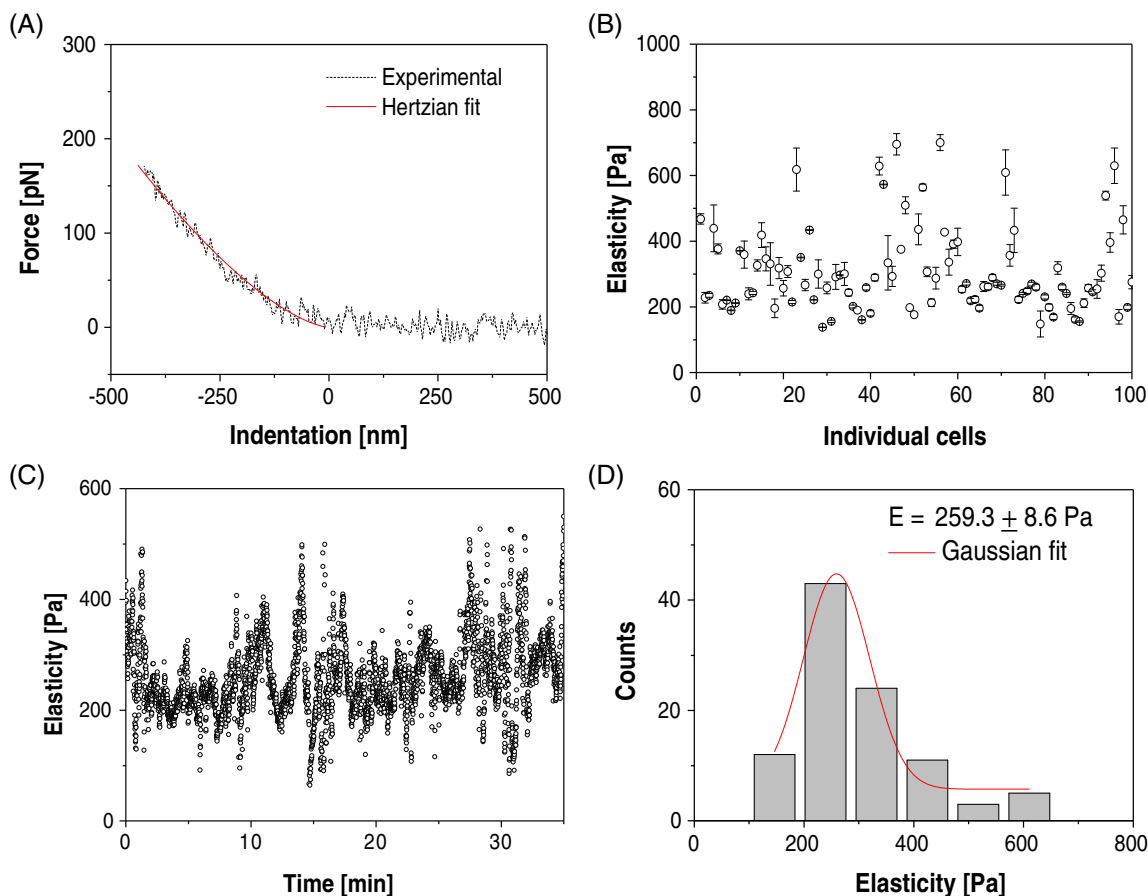


**FIGURE 2** Mechanical characteristics of the cells. A, Typical force-indentation curve (dotted line) converted from the F-D curve recorded on a cell. The curve is fitted with the Hertz model (solid line) to get cell's elasticity. B, Representative elasticity pattern showing the fluctuation of the elasticity at different time points of an individual cell. C, Elasticity with a SE of individual cells. D, Histogram showing the elasticity of the cells which is obtained by fitting the histogram with the Gaussian dispersion model (solid line)

To understand the impact of cholesterol depletion on mechanical characteristics of the cell, we incubated the cells with 10 mM M $\beta$ CD for 2 hours in cell culture conditions followed by measuring mechanical characteristics on top of the cells (Figure 3). Figure 3A is a histogram showing the elasticity of 91 cells. Applying Gaussian fit to the histogram (solid line) results in the mean cell elasticity of  $1555.5 \pm 39.5$  Pa. Applying statistical analysis with a one-way ANOVA test showed that the elasticity of the untreated cell shown in Figure 2D is significantly different from that of M $\beta$ CD treated cells with  $P < .01$ . To clarify how long the cell will respond to the appearance of the chemical, we performed elasticity measurements on top of individual cells in their physiological condition using a continuous manner and added M $\beta$ CD to the final 1 mM and 10 mM during the measurement ( $n = 3$ ). Figure 3B and C show elasticity vs time curves which show the response of the cell right after the drug is introduced into the medium. We observed that the instability of the cells suddenly increased at lower M $\beta$ CD added and increased much more at higher M $\beta$ CD added with large variation range ( $\sim 3000$  Pa). This change in cell elasticity was not observed in the case of adding the same amount of cell culture medium instead of the drug as a control into the solution during elasticity measurement (data not shown). Perhaps the amount

of cell culture medium added (1%) was too little to take effect. Figure 3D and E are histograms showing the frequency of observing elasticity before and after adding 1 and 10 mM M $\beta$ CD. They showed a significant effect of the drugs on the cell elasticity.

The difference from M $\beta$ CD, cytoD is known to disrupt the actin cytoskeleton. The response of the cells against actin depolymerization is presented in Figure 4. Figure 4A is histogram showing elasticity of 103 cells after being treated by 10  $\mu$ M cytoD. Fitting the histogram with the Gaussian distribution model results in cell elasticity of  $173.8 \pm 5.9$  Pa. This result is approximately equal to 2/3 elasticity value of the untreated cell. To investigate the influence of this drug on the cellular mechanics, we performed similar nanoindentation measurements as in the case of M $\beta$ CD, that is, adding cytoD into the medium to the final concentration of 10  $\mu$ M while measuring the force curves on an untreated cell ( $n = 3$ ). Figure 4B and C show elasticity vs time curves before and after adding 1 and 10  $\mu$ M cytoD, respectively. The elasticity patterns show that at 1  $\mu$ M cytoD, cell stability increased, and the median elasticity was slightly changed while the cell elasticity was rapidly decreased after adding 10  $\mu$ M cytoD. The variation range of the cell elasticity after 10  $\mu$ M cytoD treatment is  $\sim 250$  Pa which is in the variation range of the untreated cells. The median elasticity of the

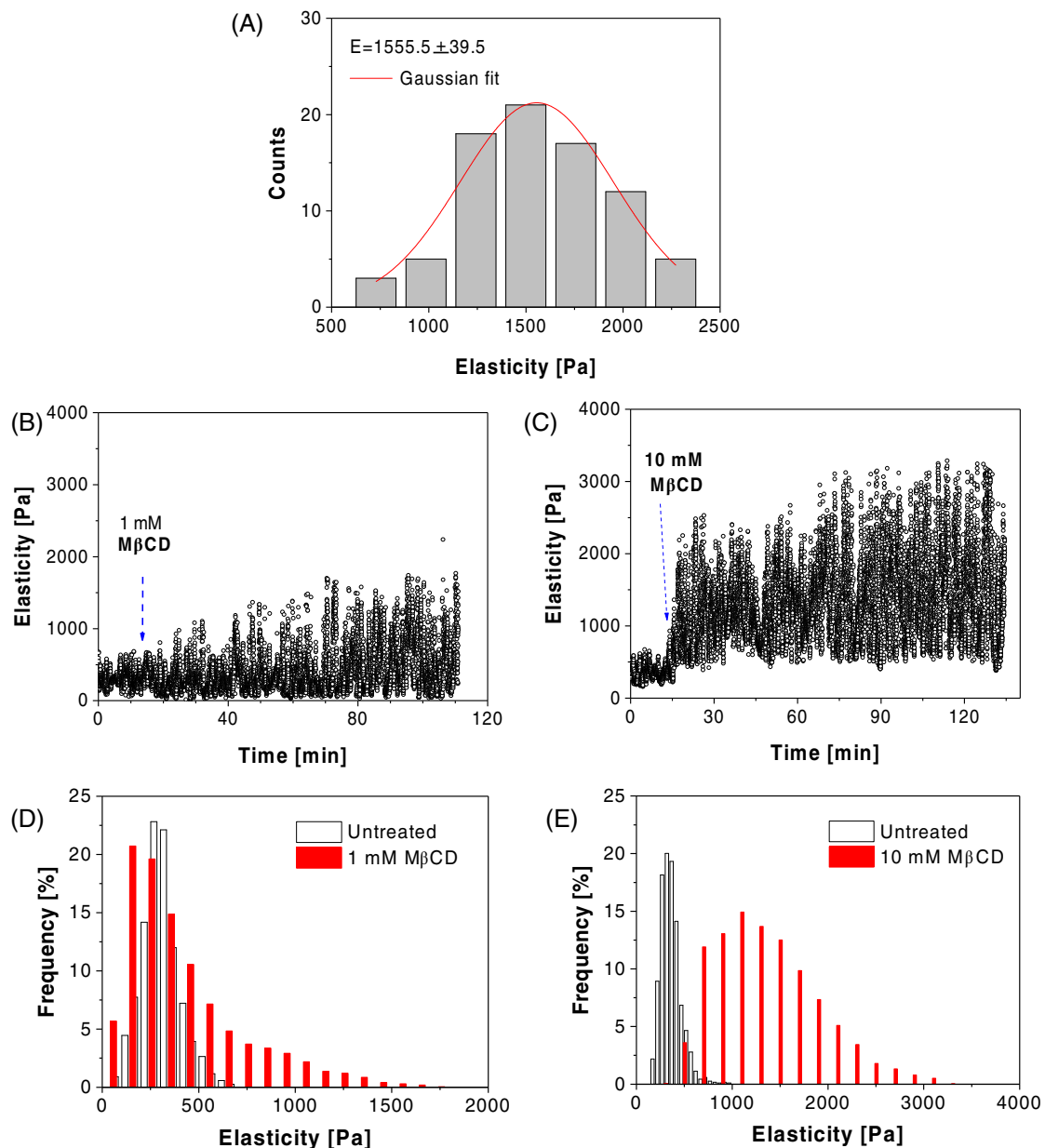


**FIGURE 3** MβCD-induced changes in cellular mechanics. A, Histogram fitted with the Gaussian dispersion model (solid lines) that shows the elasticity of the cells. B, C Elasticity profiles showing the mechanical response of the cells before and after adding 1 mM B, and 10 mM C, MβCD. Dashed arrows point to the time point the MβCD was added. D, E corresponding histograms showing frequency of observing elasticity before and after (red) MβCD treatments

treated cell remains stable for more than 80 minutes and is smaller than that of the untreated cell. Figure 4D and E are histograms showing a frequency of observing elasticity before and after adding 1 and 10  $\mu$ M cytoD. They showed a certain effect of the drugs on the cell elasticity.

#### 4 | DISCUSSION

We examined the elasticity of HEK cells proliferating singly on the glass surface by applying a very low loading force so that the

indentation depth did not exceed 10% of the cell height. This was to minimize the complication of the underlying hard surface.<sup>36</sup> However, this effect should still be taken into account. Applying correction of Hertz model by Dimitriadis *et al.*<sup>37</sup> showed that when indenting HEK cells with a 4.2- $\mu$ m-diameter tip, the apparent modulus is overestimated by 8% for a modulus of 259 Pa and 11% for a modulus of 1555 Pa. This effect is less prominent for pyramidal tips when used with the Hertz model if the tip creates local strains that do not exceed the linear-elastic assumption. However, this geometry overestimated elasticity by 60% when compared to that found with a spherical tip.<sup>37</sup> The Hertz model fits well with the data, but still, there are errors in

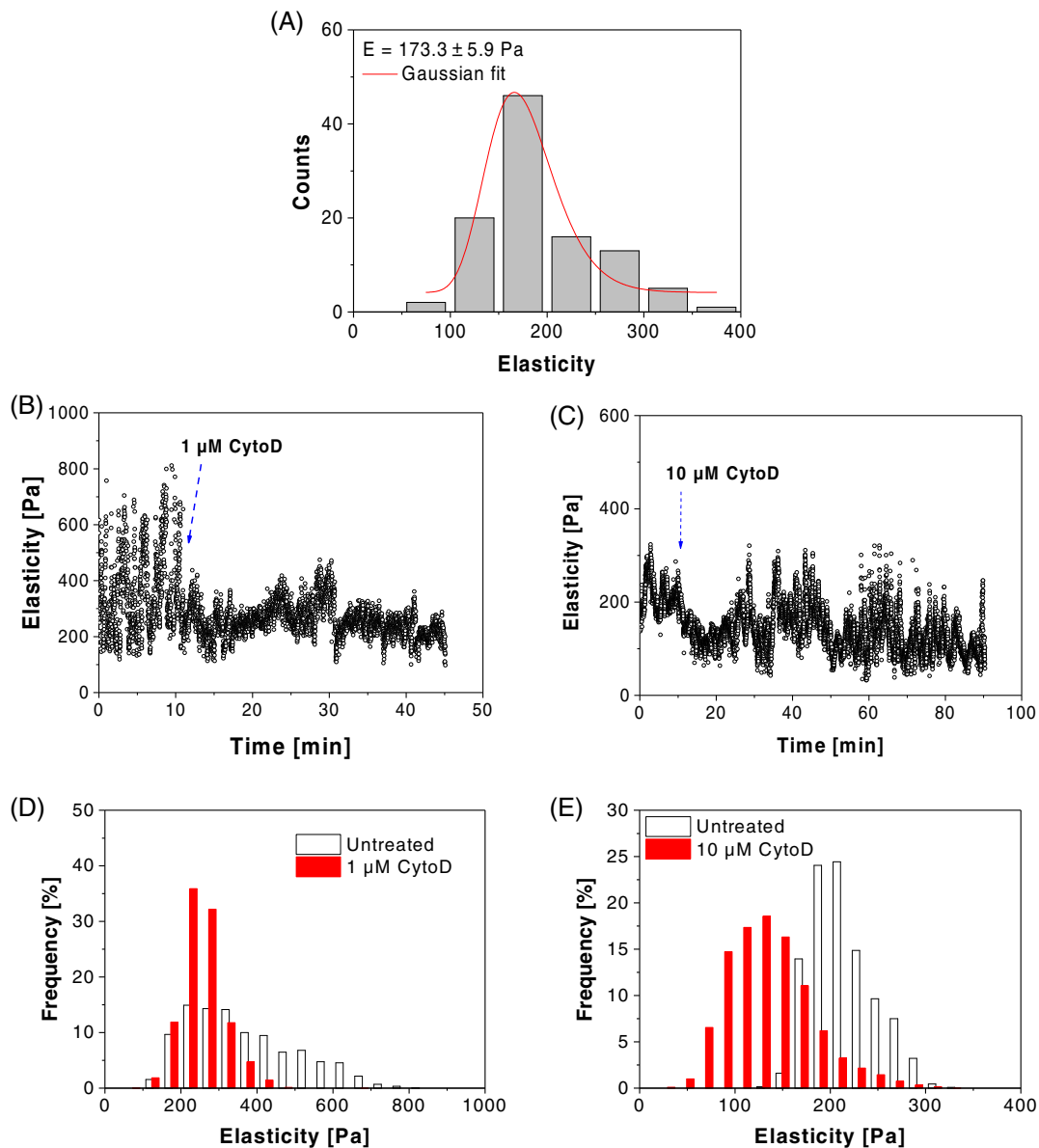


**FIGURE 4** Impact of cytoD on cellular mechanics. A, Histogram showing the mean elasticity of the cells treated with cytoD after 30 minutes. The solid line is a Gaussian fit to the data. B, C Elasticity profiles showing changes in the cell elasticity when 1  $\mu$ M B and 10  $\mu$ M C cytoD were added during nanoindentation measurement on untreated cells. Dashed arrows point to the time point cytoD was added. D, E Corresponding histograms showing frequency of observing elasticity before and after cytoD (red) treatments

the absolute value of elasticity when using this model for the estimation of Young's modulus. This is because this model is applied to homogeneous and isotropic materials while HEK cells, like other cell lines, have a membrane, cytoskeleton, nucleus, and organelles that make them inhomogeneous. Regardless of the errors, the Hertz model remains the main approach to estimate the elasticity of cells. The cell elasticity in the current study is twice lower than that observed previously where cells were proliferating in large confluent.<sup>14</sup> This means that those cells had been cultured in high density so they had to proliferate in a narrow space. This condition made the cells inflated due to a compression of the surrounding cells leading to a tension over the whole cell surface which might result in higher elasticity like in the case

of cell rounding.<sup>29</sup> Current result also shows lower elasticity value than that observed by Kagiwada *et al.*<sup>33</sup> This may be due to the effect of the tip geometry and other issues related to AFM technique.<sup>38</sup>

It is well known that cell surface tension and bending modulus increased while the amplitude of membrane-cytoskeleton fluctuation decreased during cholesterol sequestration leading to cell stiffening.<sup>27,39</sup> It is reported that if cells are incubated with 5–10 mM M $\beta$ CD for more than 2 hours, 80–90% of total cellular cholesterol will efficiently be extracted and the number of microvilli will be greatly reduced.<sup>40,41</sup> It is also showed that cholesterol depletion will impair several cytoskeleton-dependent cellular functions, such as cell motility, polarization, and migration.<sup>42–44</sup> Here, we observed that the cells

were significantly stiffened when lipid rafts were disrupted by cholesterol depletion. This may be due to the change in the properties of the submembrane F-actin or its attachment to the membrane, which is central to a series of cellular responses. Therefore, our observation suggested that depletion of cholesterol level stabilizes the submembrane cytoskeleton<sup>45</sup> and enhances the mechanical scaffold of the cell membrane, rather than uncouples the plasma membrane from the submembrane cytoskeleton.<sup>23</sup> The observed increase in the cell stiffness may be either regulated by Rho-GTPases, that have been reported to partition into lipid rafts<sup>46</sup> or due to an affection of cholesterol depletion on actin stability by sequestering of PIP<sub>2</sub>.<sup>45</sup> To gain a more precise measure of how long cells respond to the appearance of M $\beta$ CD in their physiological condition, we added this chemical to the solution while performing nanoindentation measurements on individually untreated cells. We observed that individual cells responded immediately upon detecting this drug in their living conditions as evidenced by a sudden increase in their elasticity with a large mechanical variation range. This suggested that the extraction of cholesterol occurred right after cells detect M $\beta$ CD and the depletion process might require less incubation time than 2 hours. These variations in membrane mechanics may be due to the rearrangement of the actin cytoskeleton and stress fiber formation as previously described.<sup>27</sup>

It is important to note that the increase in cell stiffness may be a consequence of cholesterol-dependent changes in the properties of the actomyosin cortex whose full function is maintaining tension in the cortex.<sup>39</sup> To investigate the impact of actomyosin integrity on the cell surface tension, we incubated the cells with cytoD which is known to promote disruption of the F-actin filaments. We observed that the depolymerization of the actin cytoskeleton induced a decrease in cell elasticity. It should be noted that even actin filaments are disrupted, cell membrane still attaches to multiple cytoskeleton proteins and the membrane stiffness is still dominated by the cytoskeleton.<sup>23</sup> It is apparent that coupling between the cortical cytoskeleton and the cell membrane helps maintain the mechanical features of the cells. The slight decrease in cell elasticity after the F-actin filaments had been disrupted suggested that the ability of contraction of the cell to respond against the chemical stimuli is reduced. To verify how single cells responding to the actin depolymerization, we added cytoD into the cell living environment while measuring the elasticity of individual cells. We observed that the cells responded immediately after detecting the appearance of this chemical like in the case of M $\beta$ CD but in an opposite way, that is, they were softened and the variation range of the cell elasticity after treatment was in the range of untreated cells and was much smaller than that stimulated by M $\beta$ CD. This suggested the disruption process of the actin cytoskeleton occurred faster than the expected incubation time.

In summary, we have reexamined the elastic modulus of single HEK cells using recommended parameters for AFM nanoindentation measurements of soft cells.<sup>35</sup> We observed that flattening of the cell membrane by cholesterol extraction significantly stiffens the cells whereas depolymerization of the actin cytoskeleton softens the cells. The mechanical response of the cells against these pharmaceutical stimuli may be interpreted in terms of cell shape remodeling and

actomyosin-mediated contraction. We introduced here a simple approach to directly tract the mechanical responses of the cells in real-time with high temporal resolution. Our approach may be applied to characterize other biological systems like yeast or bacteria and may be helpful for the development of cell biology.

## ACKNOWLEDGEMENTS

This work was supported by grants from the German Federal Ministry of Education and Research (BMBF, FKZ 03Z2CN12) and the German Research Foundation (DFG, NG 133/1-2).

## AUTHOR CONTRIBUTIONS

V.C.B. designed the research study. V.C.B and T.H.N. contributed essential reagents or tools, analyzed the data, and wrote the manuscript.

## ORCID

Thi-Huong Nguyen  <https://orcid.org/0000-0002-9237-3482>

## REFERENCES

1. Laurent VM, Kasas S, Yersin A, et al. *Gradient of rigidity in the lamellipodia of migrating cells revealed by atomic force microscopy*. *Biophys J*. 2005;89:667-675. <https://doi.org/10.1529/biophysj.104.052316>.
2. Nagayama M, Haga H, Kawabata K. *Drastic change of local stiffness distribution correlating to cell migration in living fibroblasts*. *Cell Motil Cytoskeleton*. 2001;50:173-179. <https://doi.org/10.1002/cm.10008>.
3. Bui VC, Nguyen TH. *Biophysical characteristics of hematopoietic cells during division*. *Exp Cell Res*. 2018;367:132-136. <https://doi.org/10.1016/j.yexcr.2018.03.026>.
4. Oberleithner H, Callies C, Kusche-Vihrog K, et al. *Potassium softens vascular endothelium and increases nitric oxide release*. *Proc Natl Acad Sci U S A*. 2009;106:2829-2834. <https://doi.org/10.1073/pnas.0813069106>.
5. Iyer S, Gaikwad RM, Subba-Rao V, Woodworth CD, Sokolov I. *Atomic force microscopy detects differences in the surface brush of normal and cancerous cells*. *Nat Nanotechnol*. 2009;4:389-393. <https://doi.org/10.1038/nnano.2009.77>.
6. Matzke R, Jacobson K, Radmacher M. *Direct, high-resolution measurement of furrow stiffening during division of adherent cells*. *Nat Cell Biol*. 2001;3:607-610. <https://doi.org/10.1038/35078583>.
7. Oberleithner H, Riethmuller C, Schillers H, MacGregor GA, de Wardener HE, Hausberg M. *Plasma sodium stiffens vascular endothelium and reduces nitric oxide release*. *Proc Natl Acad Sci U S A*. 2007;104:16281-16286. <https://doi.org/10.1073/pnas.0707791104>.
8. Guck J, Ananthakrishnan R, Moon TJ, Cunningham CC, Kas J. *Optical deformability of soft biological dielectrics*. *Phys Rev Lett*. 2000;84:5451-5454. <https://doi.org/10.1103/PhysRevLett.84.5451>.
9. Evans E, Yeung A. *Apparent viscosity and cortical tension of blood granulocytes determined by micropipet aspiration*. *Biophys J*. 1989;56:151-160. [https://doi.org/10.1016/S0006-3495\(89\)82660-8](https://doi.org/10.1016/S0006-3495(89)82660-8).
10. Binnig G, Quate CF, Gerber C. *Atomic force microscope*. *Phys Rev Lett*. 1986;56:930-933. <https://doi.org/10.1103/PhysRevLett.56.930>.
11. Collinsworth AM, Zhang S, Kraus WE, Truskey GA. *Apparent elastic modulus and hysteresis of skeletal muscle cells throughout differentiation*. *Am J Physiol Cell Physiol*. 2002;283:C1219-C1227. <https://doi.org/10.1152/ajpcell.00502.2001>.
12. Costa KD. *Imaging and probing cell mechanical properties with the atomic force microscope*. *Methods Mol Biol*. 2006;319:331-361. [https://doi.org/10.1007/978-1-59259-993-6\\_17](https://doi.org/10.1007/978-1-59259-993-6_17).
13. Hertz H. *Über die berührung fester elastischer körper*. *J Reine Angew Math*. 1881;92:156-171.

14. Bui VC, Nguyen TH. *The role of CD4 on mechanical properties of live cell membrane*. J Biomed Mater Res A. 2016;104:239-244. <https://doi.org/10.1002/jbm.a.35559>.
15. Mathur AB, Collinsworth AM, Reichert WM, Kraus WE, Truskey GA. *Endothelial, cardiac muscle and skeletal muscle exhibit different viscous and elastic properties as determined by atomic force microscopy*. J Biomech. 2001;34:1545-1553. [https://doi.org/10.1016/s0021-9290\(01\)00149-x](https://doi.org/10.1016/s0021-9290(01)00149-x).
16. Fehon RG, McClatchey AI, Bretscher A. *Organizing the cell cortex: the role of ERM proteins*. Nat Rev Mol Cell Biol. 2010;11:276-287. <https://doi.org/10.1038/nrm2866>.
17. Salbreux G, Charras G, Paluch E. *Actin cortex mechanics and cellular morphogenesis*. Trends Cell Biol. 2012;22:536-545. <https://doi.org/10.1016/j.tcb.2012.07.001>.
18. Heidemann SR, Wirtz D. *Towards a regional approach to cell mechanics*. Trends Cell Biol. 2004;14:160-166. <https://doi.org/10.1016/j.tcb.2004.02.003>.
19. Alarmo EL, Pärssinen J, Ketolainen JM, Savinainen K, Karhu R, Kallioniemi A. *BMP7 influences proliferation, migration, and invasion of breast cancer cells*. Cancer Lett. 2009;275:35-43. <https://doi.org/10.1016/j.canlet.2008.09.028>.
20. Sato K, Adachi T, Ueda D, Hojo M, Tomita Y. *Measurement of local strain on cell membrane at initiation point of calcium signaling response to applied mechanical stimulus in osteoblastic cells*. J Biomech. 2007;40:1246-1255. <https://doi.org/10.1016/j.jbiomech.2006.05.028>.
21. Voitchovsky K, Contera SA, Kamihira M, Watts A, Ryan JF. *Differential stiffness and lipid mobility in the leaflets of purple membranes*. Biophys J. 2006;90:2075-2085. <https://doi.org/10.1529/biophysj.105.072405>.
22. Yeagle PL. *Cholesterol and the cell membrane*. Biochim Biophys Acta. 1985;822:267-287. [https://doi.org/10.1016/0304-4157\(85\)90011-5](https://doi.org/10.1016/0304-4157(85)90011-5).
23. Byfield FJ, Aranda-Espinoza H, Romanenko VG, Rothblat GH, Levitan I. *Cholesterol depletion increases membrane stiffness of aortic endothelial cells*. Biophys J. 2004;87:3336-3343. <https://doi.org/10.1529/biophysj.104.040634>.
24. Gunning PW, Ghoshdastider U, Whitaker S, Popp D, Robinson RC. *The evolution of compositionally and functionally distinct Actin filaments*. J Cell Sci. 2015;128:2009-2019. <https://doi.org/10.1242/jcs.165563>.
25. Clark AG, Wartlick O, Salbreux G, Paluch EK. *Stresses at the cell surface during animal cell morphogenesis*. Curr Biol. 2014;24:R484-R494. <https://doi.org/10.1016/j.cub.2014.03.059>.
26. Cuerrier CM, Benoit M, Guillemette G, Gobeil F Jr, Grandbois M. *Real-time monitoring of angiotensin II-induced contractile response and cytoskeleton remodeling in individual cells by atomic force microscopy*. Eur J Physiol. 2009;457:1361-1372. <https://doi.org/10.1007/s00424-008-0596-0>.
27. Hissa B, Pontes B, Roma PMS, et al. *Membrane cholesterol removal changes mechanical properties of cells and induces secretion of a specific pool of lysosomes*. PLoS One. 2013;8:e82988. <https://doi.org/10.1371/journal.pone.0082988>.
28. Rotsch C, Radmacher M. *Drug-induced changes of cytoskeletal structure and mechanics in fibroblasts: an atomic force microscopy study*. Biophys J. 2000;78:520-535. [https://doi.org/10.1016/S0006-3495\(00\)76614-8](https://doi.org/10.1016/S0006-3495(00)76614-8).
29. Stewart MP, Helenius J, Toyoda Y, Ramanathan SP, Muller DJ, Hyman AA. *Hydrostatic pressure and the actomyosin cortex drive mitotic cell rounding*. Nature. 2011;469:226-230. <https://doi.org/10.1038/nature09642>.
30. Grady ME, Composto RJ, Eckmann DM. *Cell elasticity with altered cytoskeletal architectures across multiple cell types*. J Mech Behav Biomed Mater. 2016;61:197-207. <https://doi.org/10.1016/j.jmbm.2016.01.022>.
31. Schulze C, Muller K, Kas JA, Gerdemann JC. *Compaction of cell shape occurs before decrease of elasticity in CHO-K1 cells treated with actin cytoskeleton disrupting drug cytochalasin D*. Cell Motil Cytoskeleton. 2009;66:193-201. <https://doi.org/10.1002/cm.20341>.
32. Graham FL, Smiley J, Russell WC, Nairn R. *Characteristics of a human cell line transformed by DNA from human adenovirus type 5*. J Gen Virol. 1977;36:59-74. <https://doi.org/10.1099/0022-1317-36-1-59>.
33. Kagiwada H, Nakamura C, Kihara T, et al. *The mechanical properties of a cell, as determined by its Actin cytoskeleton, are important for nanoneedle insertion into a living cell*. Cytoskeleton. 2010;67:496-503. <https://doi.org/10.1002/cm.20460>.
34. Shimizu Y, Kihara T, Haghparast SM, Yuba S, Miyake J. *Simple display system of mechanical properties of cells and their dispersion*. PLoS One. 2012;7:e34305. <https://doi.org/10.1371/journal.pone.0034305>.
35. Harris AR, Charras GT. *Experimental validation of atomic force microscopy-based cell elasticity measurements*. Nanotechnology. 2011;22:345102. <https://doi.org/10.1088/0957-4484/22/34/345102>.
36. Domke J, Dannöhl S, Parak WJ, Müller O, Aicher WK, Radmacher M. *Substrate dependent differences in morphology and elasticity of living osteoblasts investigated by atomic force microscopy*. Colloids Surf B. 2000;19:367-379.
37. Dimitriadis EK, Horkay F, Maresca J, Kachar B, Chadwick RS. *Determination of elastic moduli of thin layers of soft material using the atomic force microscope*. Biophys J. 2002;82:2798-2810. [https://doi.org/10.1016/S0006-3495\(02\)75620-8](https://doi.org/10.1016/S0006-3495(02)75620-8).
38. Schillers H, Rianna C, Schäpe J, et al. *Standardized nanomechanical atomic force microscopy procedure (SNAP) for measuring soft and biological samples*. Sci Rep. 2017;7:5117. <https://doi.org/10.1038/s41598-017-05383-0>.
39. Pietuch A, Brückner BR, Fine T, Mey I, Janshoff A. *Elastic properties of cells in the context of confluent cell monolayers: impact of tension and surface area regulation*. Soft Matter. 2013;9:11490-11502. <https://doi.org/10.1039/C3SM51610E>.
40. Poole K, Meder D, Simons K, Muller D. *The effect of raft lipid depletion on microvilli formation in MDCK cells, visualized by atomic force microscopy*. FEBS Lett. 2004;565:53-58. <https://doi.org/10.1016/j.febslet.2004.03.095>.
41. Edidin M. *The state of lipid rafts: from model membranes to cells*. Annu Rev Biophys Biomol Struct. 2003;32:257-283. <https://doi.org/10.1146/annurev.biophys.32.110601.142439>.
42. Manes S et al. *Membrane raft microdomains mediate front-rear polarity in migrating cells*. EMBO J. 1999;18:6211-6220. <https://doi.org/10.1093/emboj/18.22.6211>.
43. Gomez-Mouton C, Abad JL, Mira E, et al. *Segregation of leading-edge and uropod components into specific lipid rafts during T cell polarization*. Proc Natl Acad Sci U S A. 2001;98:9642-9647. <https://doi.org/10.1073/pnas.171160298>.
44. Pierini LM, Eddy RJ, Fuortes M, Seveau S, Casulo C, Maxfield FR. *Membrane lipid organization is critical for human neutrophil polarization*. J Biol Chem. 2003;278:10831-10841. <https://doi.org/10.1074/jbc.M212386200>.
45. Kwik J, Boyle S, Fooksman D, Margolis L, Sheetz MP, Edidin M. *Membrane cholesterol, lateral mobility, and the phosphatidylinositol 4,5-bisphosphate-dependent organization of cell Actin*. Proc Natl Acad Sci U S A. 2003;100:13964-13969. <https://doi.org/10.1073/pnas.2336102100>.
46. Grimmer S, van Deurs B, Sandvig K. *Membrane ruffling and macropinocytosis in A431 cells require cholesterol*. J Cell Sci. 2002;115:2953-2962.

**How to cite this article:** Bui V-C, Nguyen T-H. Direct monitoring of drug-induced mechanical response of individual cells by atomic force microscopy. *J Mol Recognit*. 2020;33:e2847. <https://doi.org/10.1002/jmr.2847>